Environ. Sci. Technol. **2008,** *42,* 8459–8464

Modified Thermal-Optical Analysis Using Spectral Absorption Selectivity To Distinguish Black Carbon from Pyrolized Organic Carbon

ODELLE L. HADLEY,* CRAIG E. CORRIGAN, AND THOMAS W. KIRCHSTETTER

Scripps Institution of Oceanography, MC 0221, La Jolla, California 92093-0221, and Lawrence Berkeley National Laboratory, 1 Cyclotron Road, MS 70R0108B, Berkeley, California 94720

Received February 13, 2008. Revised manuscript received August 11, 2008. Accepted September 18, 2008.

This study presents a method for analyzing the black carbon (BC) mass loading on a quartz fiber filter using a modified thermal-optical analysis method, wherein light transmitted through the sample is measured over a spectral region instead of at a single wavelength. Evolution of the spectral light transmission signal depends on the relative amounts of light-absorbing BC and char, the latter of which forms when organic carbon in the sample pyrolyzes during heating. Absorption selectivities of BC and char are found to be distinct and are used to apportion the amount of light attenuated by each component in the sample. Light attenuation is converted to mass concentration on the basis of derived mass attenuation efficiencies (MAEs) of BC and char. The fractions of attenuation due to each component are scaled by their individual MAE values and added together as the total mass of light absorbing carbon (LAC). An iterative algorithm is used to find the MAE values for both BC and char that provide the best fit to the carbon mass remaining on the filter (derived from direct measurements of thermally evolved CO_2) at temperatures higher than 480 °C. This method was applied to measure the BC concentration in precipitation samples collected in northern California. The uncertainty in the measured BC concentration of samples that contained a high concentration of organics susceptible to char ranged from 12% to 100%, depending on the mass loading of BC on the filter. The lower detection limit for this method was approximately 0.35 μg of BC, and the uncertainty approached 20% for BC mass loading greater than 1.0 μg of BC.

Introduction

Analysis of atmospheric aerosol pollution is integral to achieving a better understanding of the anthropogenic influence on global and regional climate change (*1*). Aerosols and their associated feedbacks introduce some of the largest uncertainties facing climate forecasters today (*2*). Black carbon (BC), a main component of soot, represents one of the largest sources of uncertainty in quantifying the net effect of aerosols on the climate (*2*−*4*). This is due to the typically large errors associated with various BC measurement techniques. This study presents a modification to a thermo-optical analysis (TOA) method that is often used to quantify BC collected on filters, but is also subject to significant artifacts from organics present in the sample that pyrolize or char during thermal analysis. The distinctive spectral absorption properties of BC and these charred organics were used to distinguish the BC mass on the filter. This analysis method was developed specifically to analyze filtered precipitation samples, where the charred organic mass dominated the BC signal during TOA. This method is useful for any BC samples where pyrolysis of organics is a problem.

The most commonly used methods for measuring the atmospheric BC concentration involve optical or a combination of thermal and optical characterization of aerosol samples collected on filters. These methods are imperfect, in part due to the nonstandardized definition of BC. Method intercomparisons, for example, yield BC estimates that differ by as much as a factor of 7 (*5, 6*). A brief description of BC measurement strategies is included below, although detailed reviews of techniques used to measure BC in aerosols may be found elsewhere (*7*−*11*).

Filter-based optical methods determine the mass of BC on the filter from measured light absorption, or attenuation, using a modification of the Beer−Lambert law (*12*):

$$\text{BC mass} = \frac{(\text{ATN})A}{\text{MAE}} \quad (1)$$

In this application concentration times the path length is redefined as the mass of BC on the filter divided by the sample area on the filter (A). The molar absorptivity is converted to the mass attenuation (absorption) efficiency (MAE) and has units of $m^2\ g^{-1}$. For filter-based measurements, attenuation (ATN) rather than absorption is used because actual light absorption is enhanced due to light scattering inside the filter (*7*).

Experimentally determined values of MAE are influenced by several factors. The filter used to collect the BC particles can have the most significant impact. For example, a highly reflective quartz fiber filter, like that in the widely used aethalometer (*13*), scatters light to the particles and enhances approximately 2-fold the amount of light absorbed by BC compared to that absorbed by the same mass of BC suspended in air (*12, 14*). Thus, the distinction between the MAE of filter-bound BC and the mass-specific *absorption cross-section* of atmospheric BC is important. Light scattered away from the detector by nonabsorbing particles can also lead to overestimation of the MAE (*15*), whereas the apparent MAE may decrease as the filter loading of BC increases (*16*). The size and mixing state of BC particles influence the MAE of both filter-bound and atmospheric particles (*7, 17, 18*). After application of corrections for filter-induced artifacts, the published range of MAE values for BC in air at 550 nm is 5−14 $m^2\ g^{-1}$, with a central value of 7.5 + 1.2 $m^2\ g^{-1}$ (*7, 18*). For BC on a quartz fiber filter, an enhancement factor of 2 yields a range of MAE values of approximately 10−20 $m^2\ g^{-1}$.

The TOA of carbonaceous particles provides a measure of the total carbon (TC) in the sample and an estimate of how much is organic carbon (OC) versus elemental carbon (EC) (*8*). In most TOA methods, the sample is heated sequentially in inert (He) and oxidative (He/O_2 mixture) atmospheres, respectively, to volatilize and combust the sample carbon. Evolved carbonaceous material is oxidized to CO_2 or reduced to methane and quantified. Nominally, the carbon evolved during heating in the inert atmosphere is OC, whereas the carbon evolved during heating in the

* Corresponding author e-mail: ohadley@ucsd.edu; phone: (858) 534-7757; fax: (858) 822-5607.

10.1021/es800448n CCC: $40.75
Published on Web 10/21/2008

oxidative atmosphere is EC. The challenge in TOA lies in differentiating the OC and EC. Early combustion of EC in the inert phase and the formation of char (EC-like material that is refractory and light-absorbing) due to pyrolysis of OC can lead to large errors in the estimation of EC. Optical characterization of the sample by either measured transmission or reflectance of laser light is intended to monitor and correct for these sources of error. Several variations of TOA exist (*8, 10, 19, 20*), including the one employed in this study (*17*). In this TOA method, the sample is heated in O_2 only (i.e, there is no inert phase) and light transmission is used to distinguish between OC and BC. The light-absorbing, refractory carbon is referred to as BC instead of EC because optical absorbance, rather than the oxidative potential of the air in the sample chamber, is the primary indicator of the carbon type. A new variation on the TOA method is the optical characterization of the sample over a broad spectral region, as opposed to at a single wavelength, in an attempt to improve the distinction between OC and BC.

Experimental Section

Modifications were made to an existing TOA method for the purpose of determining the BC content on Tissuequartz fiber filters. BC was filtered from samples of rain and snow water collected in northern California. Sample water was pulled from the sample container through a series of three filters (sample size of 0.69 cm^2) using vacuum suction. Three filters were used to ensure efficient BC retrieval from the filtrate. The filtration efficiency was determined to be 92 ± 7% using prepared standards of known quantities of soot in water. These standards were prepared using soot generated with an inverted diffusion flame of methane and air (*16*). After this soot was exposed to ozone, it was mixed in purified water, forming a colloidal suspension.

High OC concentrations in the precipitation samples caused significant char formation on the filters during analysis and interfered with the determination of the BC mass. The TOA method used in this study included broad-band optical characterization of samples as they were heated. Differences in the spectral properties between BC and organic char were used to separate the absorption due to BC from that due to the char. Light transmission, from a white light emitting diode, over a spectral range of 400−900 nm wavelengths, was measured with an Ocean Optics (model S2000) spectrometer. For this analysis, optical properties of the sample-laden filter, combined with direct measurements of thermally evolved carbon, were used to determine the BC mass on the filter. This is the first application of spectral transmission data in separating BC from char in TOA. Future work could evaluate its utility when applied to other TOA methods. Other groups have used spectral absorption properties to separate BC generated by fossil fuel combustion from BC generated from biomass combustion (*21*).

Thermo-Optical Analysis. The mass of carbon (C_{mass}) removed from the filter over a given temperature range was computed by summing the measured CO_2 mole fractions (i.e., moles of CO_2/moles of O_2) and multiplying by the moles of O_2 that flowed through the instrument. The CO_2 mole fraction was measured using a LiCOR (model 7000) CO_2 analyzer. The moles of O_2 that flowed through the instrument over a given temperature range was determined from the O_2 flow rate (0.2 L min^{-1}), the temperature ramp rate (40 °C min^{-1}), and the temperature of the O_2. The equation used to calculate C_{mass} from measured CO_2 mole fractions is given in the Supporting Information (eq S-1). The sampling interval was 1 °C over the analysis range of 50−700 °C) (*16*). Plotting TC as a function of temperature yields the carbon thermogram (Figures 1 and 2, black line). The peaks correspond to different forms of carbon evolving at different temperatures.

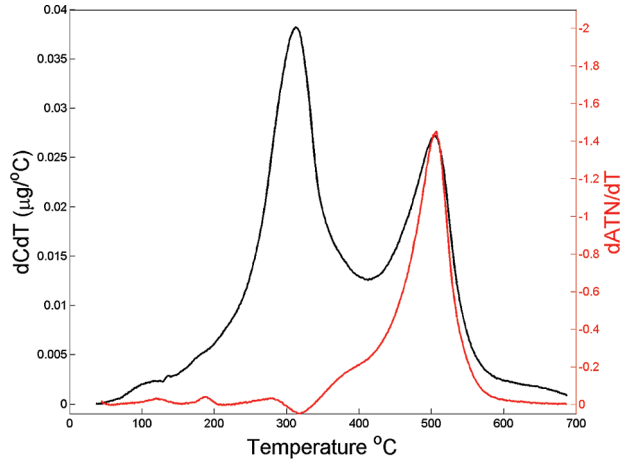

FIGURE 1. From a laboratory standard. The BC peak is at 500 °C and the organics peak at 300 °C. The red line is d(ATN)/d*T* (change in attenuation with respect to temperature), and the axis is located on the right, also in red (note the reverse axis). The black line is the change in carbon mass with respect to temperature and is calculated from evolved CO_2.

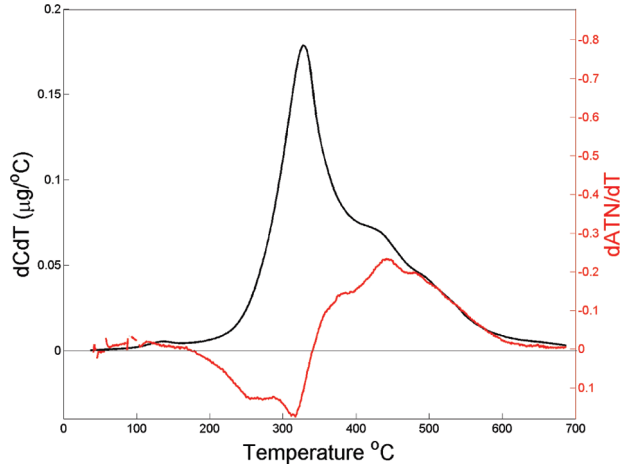

FIGURE 2. Same as Figure 1, but from a field sample of snowmelt water. Charred organics obscure the BC.

Prior work suggests that most OC evolves between 50 and 450 °C, while BC generally evolves at temperatures between 400 and 700 °C (*22*). Estimating BC and OC solely on the basis of evolution temperature, however, is error-prone because the char formed from pyrolyzed OC may coevolve with the BC. In addition, BC may combust at lower temperatures if catalytic materials are present in the sample (*22, 23*), thereby shifting the BC into the region of the thermogram dominated by OC. The recovery of carbon from filter samples was determined to be 100% ± 5% by analysis of prepared samples of potassium hydrogen phthalate and glucose (*16*).

Simultaneously measured changes in light ATN by the filter indicate the addition or removal of optically active carbon. Any wavelength of light may be used, although 550 and 880 nm are the most common. ATN(T) is determined from the transmittance of light through the filter as

$$\mathrm{ATN}(T) = -\ln\left[\frac{I_s(T)}{I_o}\frac{I_o}{I_r}\right] \qquad (2)$$

(*12, 17*), where I_o is the intensity of light incident on the filter, $I_s(T)$ is the intensity of light passing through the filter and is a function of temperature as light absorbing carbon is added and removed from the filter, and I_r is the light intensity

measured at $T = 700$ °C, when all light-absorbing carbon has been removed from the filter. A plot of the variation in ATN (i.e, the derivative of ATN with respect to temperature) versus temperature yields the optical thermogram (Figures 1 and 2, red line). When char formation is minimal and the sample does not darken during analysis (as evidenced by little or no decrease below the baseline in the optical thermogram), the black carbon and ATN thermogram peaks overlap (Figure 1) and the optical thermogram can be used to estimate the BC content of the sample. Figure 1 shows carbon and optical thermograms for a sample of particles generated with the laboratory diffusion flame (*16*). The optical thermogram may be scaled to the height of the carbon thermogram. The scaling factor is the MAE of the BC and varies with the sample.

For many samples, the left side of the BC thermogram peak may be obscured by coevolving carbonaceous material, such as refractory organics or char formed by pyrolysis of organics during analysis (Figure 2). When this occurs, it is unclear which region of the carbon thermogram to integrate for the BC mass. Integrating the carbon thermogram after the attenuation (which initially increased due to charring organics) returns to its original value overestimates the amount of BC in the sample. This is because a small amount of BC may evolve before attenuation returns to its initial value. As the measured MAE for char was typically much smaller than the MAE for BC, the BC removal will have a much greater effect on reducing attenuation than the same amount of char. After attenuation returns to initial values, a significant mass of char still residing on the filter will be interpreted as BC in the thermogram. Spectral-optical characterization of the sample can be used to aid in the distinction between BC and coevolving char, as described below.

Separating Pyrolyzed (Charred) Organic Carbon from Black Carbon. The dependence of absorption, or in this case, attenuation, on the wavelength, λ, is often expressed as a power law (*17, 24*):

$$\mathrm{ATN}(\lambda) = c\lambda^{-k} \tag{3}$$

where k is the absorption angstrom exponent (AAE) and c is the attenuation coefficient. Differences in the AAE values for pure BC, pure char, and the mixture of BC and char allowed the relative contributions of BC and char to the light attenuation on the filter to be determined throughout thermal processing. Direct measurements of thermally evolved CO_2 were used to determine the MAE for both BC and char, as well as provided the uncertainty in the calculated mass of BC. A more complete description of the process and subsequent error analysis follows.

The transmitted intensity of light ($500 < \lambda < 600$ nm) through a sample filter was continuously monitored throughout thermal evolution. This spectral region was not extended to longer or shorter wavelengths due to insufficient LED output below 480 nm and contamination of the light signal from the furnace heat at wavelengths greater than 600 nm for temperatures greater than 500 °C. Char typically began forming at $T = 200$ °C. As the amount of char increased on the filter, light attenuation also increased (Figure 2), as did the spectral dependence of absorption or measured AAE value (Figure 3). The total amount of light attenuated by char and BC on the filter may be approximated as the sum of the attenuation due to pure BC and that due to char. Thus, eq 3 may be rewritten as

$$\mathrm{ATN}(\lambda, T) = c_1(T)\lambda^{-k_{\mathrm{BC}}} + c_2(T)\lambda^{-k_{\mathrm{char}}} \approx c(T)\lambda^{-k_{\mathrm{m}}} \quad \text{for} \quad 500\ \mathrm{nm} \le \lambda \le 600\ \mathrm{nm} \tag{4}$$

As the sum of two exponentials does not follow a simple power law, eq 4 is an approximation that is valid only over the specified region of the spectrum as shown by the shaded gray area in Figure 4. k_{BC}, k_{char}, and k_{m} are, respectively, the AAEs of pure BC, pure char, and the measured LAC (light-absorbing carbon), i.e., BC plus char on the filter. k_{BC}, which is the AAE measured for laboratory soot between 500 and 600 nm, was 0.75 ± 0.02. The average AAE for BC in field samples was also 0.75; however, the uncertainty was higher at ±0.15. In eqs 4 and 6, k_{BC} is the measured AAE of the sample prior to thermal processing. k_{char} was measured during TOA of the "backup" filters from field sample filtration. These filters contained no BC, verified by optical measurements before and after TOA, and thus, attenuation changes during thermal processing were due only to charring OC. k_{char} was 5 ± 1. To determine the AAE value of the combined BC and char, or k_{m}, linear regression is used to find the slope of the log of the measured attenuation with respect to the log of the wavelength between 500 and 600 nm and at each temperature:

$$k_{\mathrm{m}}(T) = -\frac{\Delta \ln(\mathrm{ATN}(\lambda, T))}{\Delta \ln(\lambda)} \tag{5}$$

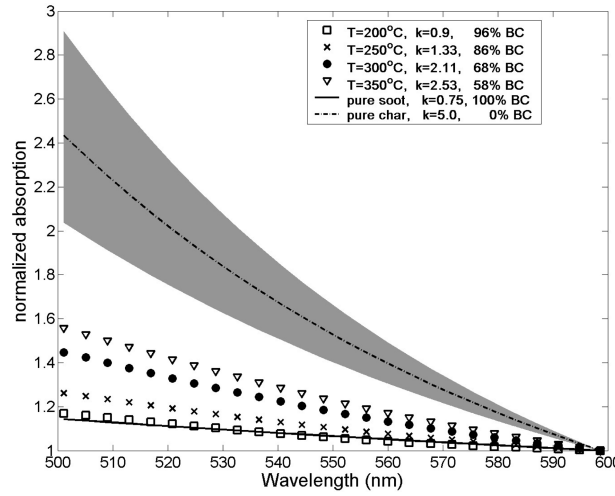

FIGURE 3. Spectral dependence of light absorption by soot and by char. The angstrom exponent, *k*, describes the change in absorption as a function of the wavelength (abs = λ^{-k}). Absorption is normalized to 600 nm. *T* refers to temperature. The shaded gray area represents the uncertainty in k_{char}.

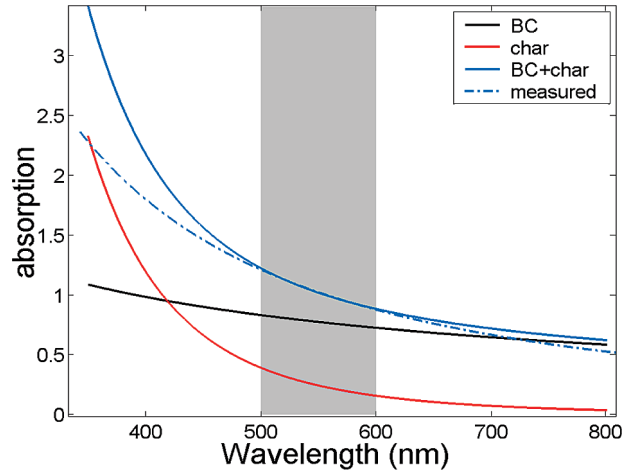

FIGURE 4. The black and red lines are the spectral absorption of pure BC and char, respectively, and follow the equation abs = $C\lambda^{-k}$, where *k* for BC is 0.75 and *k* for char is 5. *C* is determined uniquely for BC and char. The blue solid line is the summation of BC and char (red and black lines). The blue dashed line is created from the measured values for *k* and *C* between 500 and 600 nm (the shaded region).

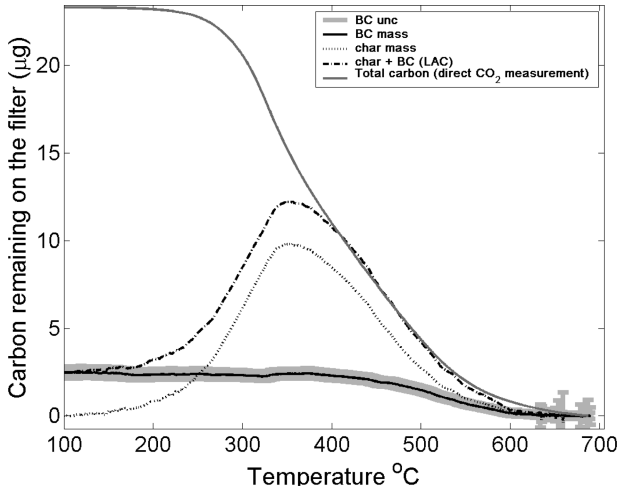

FIGURE 5. BC and char contribution to total light-absorbing carbon. Total carbon is the total amount of carbon remaining on the filter and was derived from the direct measurement of evolved CO_2 as a function of the temperature.

The attenuation constant, c, which is solved for eq 4 once k_m is known, depends directly on the mass of light-absorbing carbon on the filter and is therefore a function of temperature. Finally, solutions for c_1 and c_2 were determined using two values of λ near 550 nm ($\lambda_1 = 530$ nm and $\lambda_2 = 570$ nm). Thus, eq 4 was converted into two equations, and the two unknown constants c_1 and c_2 were solved algebraically (see the Supporting Information).

Figure 4 illustrates how solutions for c_1 and c_2 are applicable over the specified spectral region, but underpredict the absorption at shorter wavelengths. This phenomenon has been previously observed in field measurements of soot and organic carbon mixtures (*17, 24*). These equations further imply that derived AAE values for field samples, which would typically be a mix of absorbers, are valid only over the spectral region measured, and extrapolating the absorption at longer or shorter wavelengths may not be appropriate. The fraction of attenuation change at 550 nm due to BC (a) and that due to char ($1 - a$) at each temperature during thermal optical analysis, was calculated from eq 4 as

$$a(\lambda_{550\text{ nm}}, T) = \frac{c_1(T)\lambda_{550\text{ nm}}^{-k_{BC}}}{c(T)\lambda_{550\text{ nm}}^{-k_m}} \quad (6)$$

Assuming that all of the carbon evolved at temperatures greater than 480 °C was absorbing and comprised of the original BC and the char, MAE values for BC and char were determined using a best fit to the direct carbon measurement at temperatures greater than 480 °C. Previous studies have shown that nonabsorbing organic carbon evolves at temperatures below 500 °C; carbonate, also nonabsorbing, evolves at temperatures greater than 800 °C. An iterative routine was used to find MAE_{BC} and MAE_{char}, such that when the BC and char attenuation components were individually scaled by these values and summed, the reconstructed curve matched the direct measurement of carbon mass remaining on the filter (eq 7) at temperatures greater than 480 °C (Figure 5). The carbon mass on the filter was determined using the evolved carbon mass from CO_2 measurements (eq S.1, Supporting Information). The first term represents the total amount of carbon evolved from the filter, and the second term is the amount of carbon evolved between 50 °C and each 1 °C temperature increase.

$$C(T)_{\text{filter}} = \sum_{T=50}^{700} C_{\text{mass}} - \sum_{i=50}^{T} C_{\text{mass}}(i) \quad (7)$$

The range of previously published MAE values for BC on quartz fiber filters constrained the values for MAE_{BC} between 10 and 20 $m^2\ g^{-1}$. The range of values for MAE_{char}, 0.5−7 m^2/g, was found using the same backup filters used to find k_{char}. The fitting algorithm cycled through the range of MAE values at increasing increments of 0.05 $m^2\ g^{-1}$ and found those values corresponding to the minimum rms (root-mean-square) difference between the measured carbon mass and the reconstructed sum of the BC and char masses. The BC mass remaining on the filter during TOA was determined by combining the Beer−Lambert law as shown in eq 1 with the derived fraction of attenuation due to BC calculated using eq 6 and the MAE_{BC} value corresponding to the best fit with the directly measured carbon mass:

$$\text{BC mass}(T) = \frac{a_{550\text{ nm}}(T)\ \text{ATN}_{550\text{ nm}}(T)\ A}{\text{MAE}_{BC}} \quad (8)$$

Results and Discussion

The average calculated mass attenuation efficiency for the BC filtered from 29 precipitation samples was $13.97 \pm 4.2\ m^2\ g^{-1}$. This wide range of MAE values is likely due to variability in the source, chemical structure, and size of the BC particles, as well as changes in the absorption efficiency due to filter loading effects (*16*). Absorption enhancement due to coating of the BC particles by sulfates and organics (*18*) would not apply here as the water-soluble coating should be removed by the water sample. This may also explain why the MAE values tend to be on the lower end of published values for BC MAE on a scattering filter. The average calculated MAE of char was $3.1 \pm 2.3\ m^2\ g^{-1}$. The difference between the MAE for BC and that for char has important implications for BC retrievals using traditional TOA. Table 1 compares the BC mass retrieved using the TOA method described in this paper with one that assumes the MAEs of char and BC are the same. This is an assumption common to the widely used TOA methods (*8, 20, 25*). This table shows that the magnitude of the char bias can result in an overprediction of the BC mass by over a factor of 6 when the MAEs of char and BC are assumed to be the same.

An rms difference was calculated from the closeness of the fit between the reconstructed LAC (BC plus char) mass and the direct measurement of the total carbon mass from evolved CO_2 at temperatures greater than 480 °C. The rms difference, which represents the uncertainty in the BC mass, was assumed to be entirely due to the uncertainty in the MAE_{BC}, as opposed to uncertainties in the carbon measurement or the MAE of char. The uncertainty in the MAE_{BC} for each sample can be expressed as a simple calculation:

$$\sigma_{\text{MAE}_{BC}} = \left|\frac{\text{d}(\text{MAE}_{BC})}{\text{d}(\text{BC mass})}\right|(\text{rms}) \quad (9)$$

The uncertainty in a, calculated from the uncertainties in the derived values for k_{BC}, k_{char}, and k_m, and the uncertainty in the measured attenuation (± 3) and MAE_{BC} are propagated through eq 8 and give an uncertainty of the BC mass at each temperature. The overall uncertainty in the final calculation for the BC mass is the sum of the standard deviation from the retrieved BC mass between $T = 100$ °C and $T = 300$ °C and the average calculated uncertainty over the same temperature range. Figure 6 shows the percent uncertainty plotted as a function of the total BC mass on the filter. The lower detection limit for this method is approximately 0.35 μg of BC. Application of our method to the analysis of samples containing OC that charred, and no BC, did not interpret the char as BC. For BC mass greater than 1.0 μg, the percent uncertainty approaches 20%. The overall uncertainty is unique for each sample and ranges from 12% to 100%, depending on the BC concentration and char and dust contents.

TABLE 1. TOA BC Mass Retrieval (Which Assumes the Same MAE for Char and for BC) vs the BC Mass Retrieval from Modified Analysis[a]

total carbon mass (μg)	TOA BC mass (μg)	OC mass (μg)	modified BC mass (μg)	uncertainty (μg)	OC char mass (μg)	OC mass (μg)	diff (%)
29.25	4.02	25.23	1.46	0.19	8.5	19.29	−175.342
15.12	1.64	13.48	1.01	0.3	3.58	10.53	−62.3762
25.08	3.37	21.71	0.88	0.17	8.32	15.88	−282.955
26.48	3.27	23.21	1.5	0.39	8.78	16.20	−118
36.60	3.29	33.31	1.07	0.28	15.87	19.66	−207.477
43.65	4.17	39.48	0.64	0.18	13.77	29.24	−551.563
27.50	1.23	26.27	0.44	0.16	16.8	10.26	−179.545
23.30	4.1	19.20	2.39	0.33	10.67	10.24	−71.5481
54.8	2.24	52.56	1.84	0.57	12.55	40.41	−21.7391
38.05	1.26	36.79	1.11	0.39	11.47	25.47	−13.5135

[a] BC was filtered from melted snow samples collected at Lassen Volcano National Park and the Central Sierra Snow Laboratory, California, in March 2006. The sample size ranged from 75 to 200 mL.

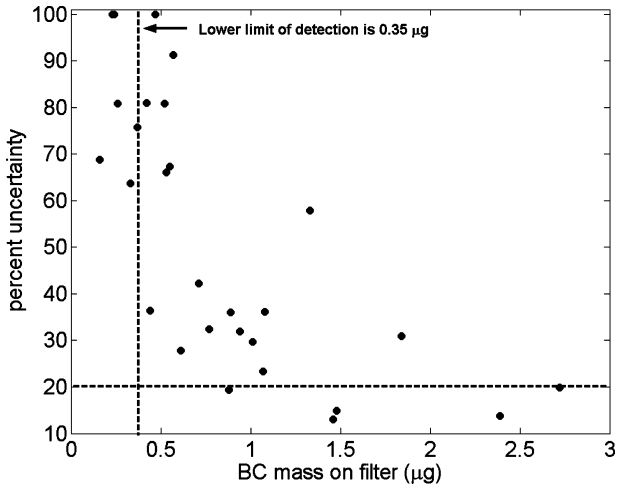

FIGURE 6. Percent uncertainty for field samples vs the filter loading. Dashed lines indicate that the uncertainty approaches a constant value of 20% for BC mass above 1.0 μg and that the lower limit of detection is 0.35 μg of BC.

During thermal processing, some inorganic material may contribute to changes in the light transmission. For example, oxidation of metals in the dust, such as Fe(II) to Fe(III), may affect light absorption measurements at visible wavelengths; however, the MAE of dust is a factor of 100 less than the MAE of BC (*26*). Consequently, the signal interference of oxidizing metals on BC should be negligible in most field samples. If the field sample does contain a high enough concentration of metals relative to the BC concentration, the oxidation of these metals at high temperatures could significantly increase the absorption of visible wavelengths at temperatures greater than 500 °C and contaminate the reference transmission, as well as obscure the AAE measurements. This effect was observed to varying degrees in a few of the field samples used in this study, which were subsequently removed from this analysis. Comparing the transmission measurement of dust-laden samples prior to and after thermal processing revealed that enhanced absorption in the visible wavelengths did not extend past 800 nm. Thus, for cases where dust contamination is severe, the change in attenuation at 880 nm may still be used to estimate the BC mass using optical methods.

Although there is still significant error associated with the BC measurement, this new analysis method provides a way to separate the BC signal from the charring signal of organics, a significant source of error in TOA. Uncertainties approach 20% when the BC mass loading exceeds 1 μg, lower than previously published uncertainties (30% and 50%) for the BC mass measured in snow and rainwater (*8, 25, 27*). This approach provides a way to characterize measurement-dependent uncertainties for each discrete sample, rather than assigning an uncertainty estimate to an entire analytical procedure. The MAE used for BC and for char result in mass calculations that, when summed, are consistent with the direct measure of total carbon mass obtained from the thermo-optical analyzer.

Relative to TOA of BC in atmospheric aerosols, the charring of organics from precipitation samples presented much higher signal interference in both thermally dependent direct measurement of carbon and optically inferred calculations. An analysis of light attenuation over a specific spectral region, rather than at a single wavelength, has led to a method for separating the BC mass from organic char using individual absorption angstrom exponent values. Applying direct carbon measurements from evolved CO_2 helped constrain and validate the MAE values obtained and used to find the BC concentration for each individual sample. In our study, an AAE value of -5 ± 1 was measured and used for char. The AAE of char produced in other common TOA methods (*8, 20*), which heat samples in helium instead of oxygen, may be different.

The techniques described above may also be applied to measurements of BC in ambient aerosol analysis. Further development of this method may allow for determining relative source contributions to BC aerosol from biomass burning and urban processes. Previous work has shown that the spectral dependence of absorption by BC particles generated by these processes differs similarly to that of BC and char. Soot generated from fossil fuel burning and urban processes has AAE values very close to that of the pure laboratory BC, while biomass burning produces soot containing spectral characteristics analogous to those of the char (*17, 21, 24*). The general applicability of the method presented in this study could be evaluated in future work by analysis of other types of samples, such as biomass smoke that contains appreciable amounts of light-absorbing organic carbon in addition to black carbon.

Acknowledgments

We thank Guido Franco and the California Energy Commission for their support (CEC Award No. MR-06-01B). We also thank Prof. T. Novakov and Jefferey Aguiar for advice and assistance during the laboratory phase of this study.

Supporting Information Available

Additional equations used in the analysis and a list of symbols and abbreviations. This information is available free of charge via the Internet at http://pubs.acs.org.

Literature Cited

(1) Penner, J. E.; Andreae, M.; Annegarn, H.; Barrie, L.; Feichter, J.; Hegg, D.; Jayaraman, A.; Leaitch, R.; Murphy, D.; Nganga, J.; Pitari, G. Aerosols, their direct and indirect effects. In *Climate Change 2001: The Scientific Basis. Contribution of Working Group I to the Third Assessment Report of the Intergovernmental Panel on Climate Change*; Houghton, J. T., Ding, Y., Griggs, D. J., Noguer, M., Linden, P. J. v. d., Dai, X., Maskell, K., Johnson, C. A., Eds.; Cambridge University Press: Cambridge, U.K., New York, 2001; pp 289−348.

(2) Ramaswamy, V.; Boucher, O.; Haigh, J.; Hauglustaine, D.; Haywood, J.; Myhre, G.; Nakajima, T.; Shi, G. Y.; Solomon, S. Radiative forcing of climate change. In *Climate Change 2001: The Scientific Basis. Contribution of Working Group I to the Third Assessment Report of the Intergovernmental Panel on Climate Change*; Houghton, J. T., Ding, Y., Griggs, D. J., Noguer, M., Linden, P. J. v. d., Dai, X., Maskell, K., Johnson, C. A., Eds.; Cambridge University Press: Cambridge, U.K., New York, 2001; pp 351−416.

(3) Jacobson, M. Z. Strong radiative heating due to the mixing state of black carbon in atmospheric aerosols. *Nature* **2001**, *409* (6821), 695–697.

(4) Penner, J. E.; Zhang, S. Y.; Chuang, C. C. Soot and smoke aerosol may not warm climate. *J. Geophys. Res., [Atmos.]* **2003**, *108* (D21), 4657, DOI:10.1029/2003JD003409.

(5) Watson, J. G.; Chow, J.; Chen, L. W. A. Summary of organic and elemental carbon/black carbon analysis methods and intercomparisons. *Aerosol Air Qual. Res.* **2005**, *5* (1), 65–102.

(6) Currie, L. A.; Benner, B. A.; Kessler, J. D.; Klinedinst, D. B.; Klouda, G. A.; Marolf, J. V.; Slater, J. F.; Wise, S. A.; Cachier, H.; Cary, R.; Chow, J. C.; Watson, J.; Druffel, E. R. M.; Masiello, C. A.; Eglinton, T. I.; Pearson, A.; Reddy, C. M.; Gustafsson, O.; Quinn, J. G.; Hartmann, P. C.; Hedges, J. I.; Prentice, K. M.; Kirchstetter, T. W.; Novakov, T.; Puxbaum, H.; Schmid, H. A critical evaluation of interlaboratory data on total, elemental, and isotopic carbon in the carbonaceous particle reference material, NIST SRM 1649a. *J. Res. Natl. Inst. Stand. Technol.* **2002**, *107* (3), 279–298.

(7) Bond, T. C.; Bergstrom, R. W. Light absorption by carbonaceous particles: An investigative review. *Aerosol Sci. Technol.* **2006**, *40* (1), 27–67.

(8) Chow, J. C.; Watson, J. G.; Chen, L. W. A.; Arnott, W. P.; Moosmuller, H. Equivalence of elemental carbon by thermal/optical reflectance and transmittance with different temperature protocols. *Environ. Sci. Technol.* **2004**, *38* (16), 4414–4422.

(9) Hitzenberger, R.; Petzold, A.; Bauer, H.; Ctyroky, P.; Pouresmaeil, P.; Laskus, L.; Puxbaum, H. Intercomparison of thermal and optical measurement methods for elemental carbon and black carbon at an urban location. *Environ. Sci. Technol.* **2006**, *40* (20), 6377–6383.

(10) Petzold, A.; Niessner, R. Method comparison study on soot-selective techniques. *Mikrochim. Acta* **1995**, *117* (3−4), 215–237.

(11) Reisinger, P.; Wonaschutz, A.; Hitzenberger, R.; Petzold, A.; Bauer, H.; Jankowski, N.; Puxbaum, H.; Chi, X.; Maenhaut, W. Intercomparison of measurement techniques for black or elemental carbon under urban background conditions in wintertime: Influence of biomass combustion. *Environ. Sci. Technol.* **2008**, *42* (3), 884–889.

(12) Weingartner, E.; Saathoff, H.; Schnaiter, M.; Streit, N.; Bitnar, B.; Baltensperger, U. Absorption of light by soot particles: Determination of the absorption coefficient by means of aethalometers. *J. Aerosol Sci.* **2003**, *34* (10), 1445–1463.

(13) Hansen, A. D. A. *The Aethalometer*; Magee Scientific Co.: Berkely, CA, 2003.

(14) Bodhaine, B. A. Aerosol absorption-measurements at Barrow, Mauna-Loa and the South-Pole. *J. Geophys. Res., [Atmos.]* **1995**, *100* (D5), 8967–8975.

(15) Arnott, W. P.; Hamasha, K.; Moosmuller, H.; Sheridan, P. J.; Ogren, J. A. Towards aerosol light-absorption measurements with a 7-wavelength aethalometer: Evaluation with a photoacoustic instrument and 3-wavelength nephelometer. *Aerosol Sci. Technol.* **2005**, *39* (1), 17–29.

(16) Kirchstetter, T. W.; Novakov, T. Controlled generation of black carbon particles from a diffusion flame and applications in evaluating black carbon measurement methods. *Atmos. Environ.* **2007**, *41* (9), 1874–1888.

(17) Kirchstetter, T. W.; Novakov, T.; Hobbs, P. V. Evidence that the spectral dependence of light absorption by aerosols is affected by organic carbon. *J. Geophys. Res., [Atmos.]* **2004**, *109* (D21), D21208, DOI: 10.1029/2004JD004999.

(18) Liousse, C.; Cachier, H.; Jennings, S. G. Optical and thermal measurements of black carbon aerosol content in different environments—Variation of the specific attenuation cross-section, sigma (σ). *Atmos. Environ., Part A* **1993**, *27* (8), 1203–1211.

(19) Lavanchy, V. M. H.; Gaggeler, H. W.; Nyeki, S.; Baltensperger, U. Elemental carbon (EC) and black carbon (BC) measurements with a thermal method and an aethalometer at the high-alpine research station Jungfraujoch. *Atmos. Environ.* **1999**, *33* (17), 2759–2769.

(20) Birch, M. E. Analysis of carbonaceous aerosols: Interlaboratory comparison. *Analyst* **1998**, *123* (5), 851–857.

(21) Sandradewi, J.; Prevot, A. S. H.; Szidat, S.; Perron, N.; Alfarra, M. R.; Lanz, V. A.; Weingartner, E.; Baltensperger, U. Using aerosol light absorption measurements for the quantitative determination of wood burning and traffic emission contributions to particulate matter. *Environ. Sci. Technol.* **2008**, *42* (9), 3316–3323.

(22) Novakov, T.; Corrigan, C. E. Thermal characterization of biomass smoke particles. *Mikrochim. Acta* **1995**, *119* (1−2), 157–166.

(23) Mikhailov, E. F.; Vlasenko, S. S.; Podgorny, I. A.; Ramanathan, V.; Corrigan, C. E. Optical properties of soot-water drop agglomerates: An experimental study. *J. Geophys. Res., [Atmos.]* **2006**, *111* (D7), D07209, DOI:10.1029/2005JD006389.

(24) Bergstrom, R. W.; Pilewskie, P.; Russell, P. B.; Redemann, J.; Bond, T. C.; Quinn, P. K.; Sierau, B. Spectral absorption properties of atmospheric aerosols. *Atmos. Chem. Phys.* **2007**, *7*, 10669–10686.

(25) Chow, J. C.; Watson, J. G.; Crow, D.; Lowenthal, D. H.; Merrifield, T. Comparison of IMPROVE and NIOSH carbon measurements. *Aerosol Sci. Technol.* **2001**, *34* (1), 23–34.

(26) Clarke, A. D.; Shinozuka, Y.; Kapustin, V. N.; Howell, S.; Huebert, B.; Doherty, S.; Anderson, T.; Covert, D.; Anderson, J.; Hua, X.; Moore, K. G.; McNaughton, C.; Carmichael, G.; Weber, R. Size distributions and mixtures of dust and black carbon aerosol in Asian outflow: Physiochemistry and optical properties. *J. Geophys. Res., [Atmos.]* **2004**, *109* (D15), D15S09, DOI:10.1029/2003JD004378.

(27) Clarke, A. D.; Noone, K. J. Soot in the Arctic snowpack—A cause for perturbations in radiative-transfer. *Atmos. Environ.* **1985**, *19* (12), 2045–2053.

ES800448N